Experimental study of sorption kinetics of n-alkanes vapour mixtures on synthetic zeolites

[a]J. LONGAUER, [b]J. ILAVSKÝ, and [b]A. BRUNOVSKÁ

[a]*Department of Chemical Engineering, Slovak Technical University, 880 37 Bratislava*

[b]*Department of Organic Technology, Slovak Technical University, 880 37 Bratislava*

Received 5 November 1980

In this paper experimental results of sorption kinetics of a binary mixture of n-alkane vapours (n-hexane, n-heptane) in a stream of carrier gas (nitrogen) on synthetic zeolite in a continuous gradientless reactor are presented. The properties of the laboratory reactor (adsorber) used have been tested by the residence time distribution function. The concentration of the gas adsorptive has been measured by analytical method using flame ionization detector together with a digital integrator. A method of estimation of the mass of the components on the adsorbent and the kinetics of the isothermal sorption of three kinds of binary mixtures with constant ratio of partial pressures of the adsorptive components is described. The adsorption rate of the components is also related to the degree of saturation of the adsorbent surface.

Приводятся результаты экспериментального изучения кинетики сорбции бинарной смеси паров н-алканов (н-гексан, н-гептан) в токе газа-носителя (азот) на синтетическом цеолите в проточном реакторе без градиента. Свойства использованного лабораторного реактора-адсорбера были испытаны на основании функции распределения времени задержки. Качественный и количественный анализы сорбирующегося газа были выполнены с использованием датчика с ионизацией в пламени и цифрового интегратора. В работе приводятся способ и результаты определения количества адсорбированного газа и кинетики изотермической сорбции трех различных видов бинарной смеси с использованием постоянного отношения парциальных давлений компонентов адсорбата. Скорость адсорбции компонентов смеси обсуждается в отношении к степени насыщения поверхности адсорбента адсорбатом.

For experimental study of binary adsorption we have used a modification of the device, the scheme of which together with the method of measuring is given in our previous paper [1]. The principal changes concern the construction of the main part — reactor, which is schematically represented in Fig. 1.

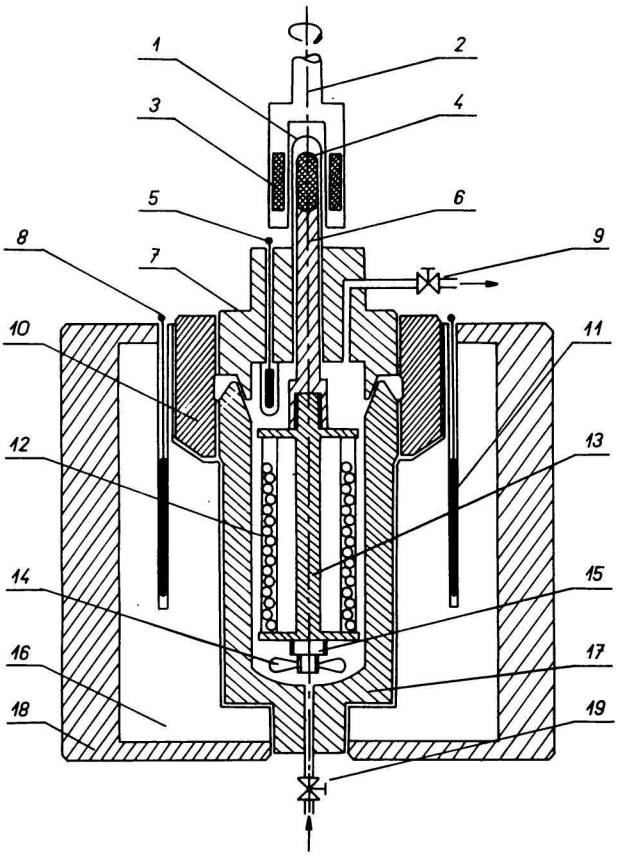

Fig. 1. Schematic section through the reactor.
1. Shaft seal; *2.* rotation magnetic pin; *3, 4.* magnetic kernel of the carrier shaft; *5.* resistance thermometer of the gas adsorptive in the reactor; *6.* shaft of the reactor; *7.* reactor lid; *8.* measurement of the temperature in the heater; *9.* shutoff valve; *10.* connecting screw chuck; *11.* resistance thermometer; *12.* bed of sample; *13.* supporter of the sample; *14.* blade stirrer; *15.* fastening spring; *16.* heater; *17.* reactor body; *18.* isolating cover; *19.* input valve.

The main advantages of this construction of the reactor are high efficiency of stirring, easy control of hydrodynamic conditions (by the change of the frequency of revolution), and safe packing.

As a test for the efficiency of stirring of the experimental reactor we have employed the closeness of its residence time distribution function to that of a perfectly stirred reactor. The results obtained by the method after [1] allow also to consider the experimental reactor to be a gradientless one. Using frequency of rotor rotation 12.5 Hz (the mean radius of rotation sorbent particle 12 mm) the

measured deviation from perfect mixing does not exceed the interval of experimental errors. The results of the study of rotation frequency *vs.* efficiency of mixing in a similar type of reactor are discussed in [1].

Owing to high efficiency of mixing, also the pressure and temperature gradients in the reactor are negligible. Due to low volumetric flow of the gas adsorptive through the reactor (of order $cm^3 s^{-1}$) during the sorption measurements, the adsorption process is very slow (6—10 h). The released heat of the adsorption can be thus reliably removed from the solid phase to the bulk stream and does not cause local overheating of the sorbent particle.

The measurements start at time $\tau = 0$, when the stream of gas adsorptive is turned over and led through the reactor to the analyzer. During the adsorption process the surface of the adsorbent is saturated by adsorbates. Simultaneously the concentration of both of the components in the gaseous stream outflowing from the reactor is increasing. The adsorption process in step one is finished, when the analyzer records equal output and input concentrations. At this moment the adsorbent surface is saturated. Afterwards the reactor is closed, the stream of the adsorptive is turned over to avoid the reactor and the concentrations of the components are raised. When the composition gets settled, the gas stream is again turned over and led through the reactor and the analyzer records the composition *vs.* time in the step two of adsorption. Similarly, the course of the adsorption is recorded in subsequent steps while the concentration of components is successively increased.

Materials

1. *Adsorbent:* spherical particles of synthetic zeolite — molecular sieve Calsit 5A. Composition (mass %): SiO_2 42%, Al_2O_3 37%, CaO 16%, Na_2O, Fe_2O_3, MgO 5%.

Mineral density	2860 kg m^{-3}
Clay contents	20%
Particle density	1148 kg m^{-3}
Diameter of particle	2.8—3.0 mm
Bulk density	710 kg m^{-3}
Specific surface	580 $m^2 g^{-1}$
Specific pore volume	0.25 $cm^3 g^{-1}$
Internal porosity	22%
Mean pore diameter	0.85 nm

The physical adsorbent parameters, as the specific surface, specific pore volume, porosity, and mean pore diameter have been determined by the gravimetric sorption method [2—4] in the Gravimat device [5].

The adsorbent sample consisted of about 90 particles of mass *ca.* 1.3 g. The histogram of distribution of particles (number of particles *vs.* diameter) is presented in Fig. 2.

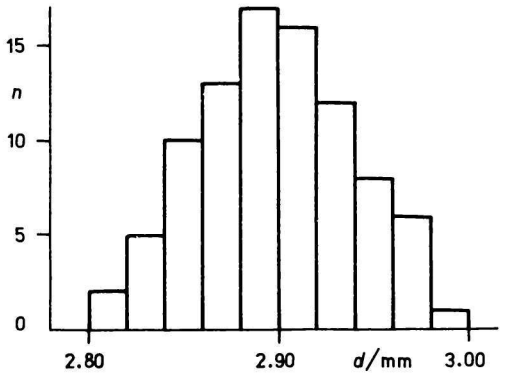

Fig. 2. Histogram of the distribution of the number of the particles n *vs.* diameter of particle d in the sample of the adsorbent.

2. *Adsorptive:* the vapour mixture of two n-alkanes (n-hexane, n-heptane) and nitrogen as a carrier gas (inert).

The vapour mixture has been prepared from pure liquid compounds of the following properties:

	n-Hexane	n-Heptane
Density at 20°C ϱ/kg m^{-3}	659.4	683.9
Boiling point at 101.3 kPa t/°C	68.7	98.4
Refractive index at 20°C	1.3749	1.3876
Minimal content of pure compounds C/mass %	99.6	99.5
Maximal content of sulfur C/mass %	0.002	0.002
Maximal content of water C/mass %	0.01	0.01

From the adsorption equilibrium measurement of carrier gas (nitrogen) under given conditions in the Gravimat device [5] we have found the mass of the adsorbed nitrogen to be negligible.

Determination of the adsorbed amount and sorption kinetics

Dependence of the mass amounts $A_i(\tau)$ of adsorbate components on the adsorbent on time is determined from the experimental time dependences of composition of gaseous stream, recorded by an analyzer during the experiment. Using the calibration curve, to each numerical value of the integrator of chromatographic peaks in particular time τ we have assigned a value of the dimensionless concentration of the components $c_i(\tau)$ of the mixture in the gas flow behind the reactor. The mass concentration of the i-th component $C_i(\tau)$ and the mass flow of the i-th component $\dot{m}_i(\tau)$ at a given flow rate of carrier gas can be

evaluated from the expression for the dimensionless concentration of the i-th component

$$c_i(\tau) = \frac{C_i(\tau) - C_{i\,0n}}{C_{i\,0} - C_{i\,0n}} \tag{1}$$

where $C_i(\tau)$ and $C_{i\,0}$ are concentrations of the i-th components in the outlet and inlet stream, respectively ($C_{i\,0}$ is time-independent due to constant input conditions during one adsorption step) and $C_{i\,0n}$ is the equilibrium concentration of the i-th component corresponding to the previous step.

The mass amount of the i-th adsorbate component on the adsorbent at time τ is determined indirectly from the material balance

$$A_i(\tau) = \int_0^\tau [\dot{m}_{i\,z}(\tau) - \dot{m}_i(\tau)]\,\mathrm{d}\tau \tag{2}$$

where $\dot{m}_{i\,z}(\tau)$ is the mass flow of the component in the outflowing stream provided no adsorption is taking place and can be determined from the measured residence time distribution function of the system $\varphi(\tau)$

$$\dot{m}_{i\,z}(\tau) = \dot{m}_{i\,0}\,\varphi(\tau) \tag{3}$$

where $\dot{m}_{i\,0}$ is the mass flow of the i-th component in the inlet flow (corresponding to the concentration $C_{i\,0}$). The experimental residence time distribution function $\varphi(\tau)$ has been measured by a stimulus—response technique using step jump as input. The dimensionless response $\varphi(\tau)$ to the step input at time $\tau = 0$ is defined by the ratio

$$\varphi(\tau) = \frac{C(\tau)}{C_0} \tag{4}$$

where $C(\tau)$ is the concentration of the tracer material at time τ in the fluid stream leaving reactor and C_0 the constant tracer concentration in the entering stream.

The experimental curve $\varphi(\tau)$ is best fitted by the analytical function

$$\varphi(\bar{\tau}) = 1 - a\bar{\tau}^b \exp(c\bar{\tau}) \tag{5}$$

where $\bar{\tau}$ is the value of time (in min) and a, b, c are constants, which for each experimental curve can be determined by the method [6]. For the following experiment conditions

reactor temperature	130°C
reactor pressure	100.4 kPa
volumetric gas flow	47.5 $cm^3 min^{-1}$
volume of the gaseous phase in the reactor	101.4 cm^3
frequency of rotor rotation	12.5 Hz

the values of constants a, b, c are: $a = 1.191$, $b = 0.219$, $c = -0.511$.

The experimental function $\varphi(\tau)$ for the three experiments and the theoretical one given by eqn (*5*) are illustrated in Fig. 3.

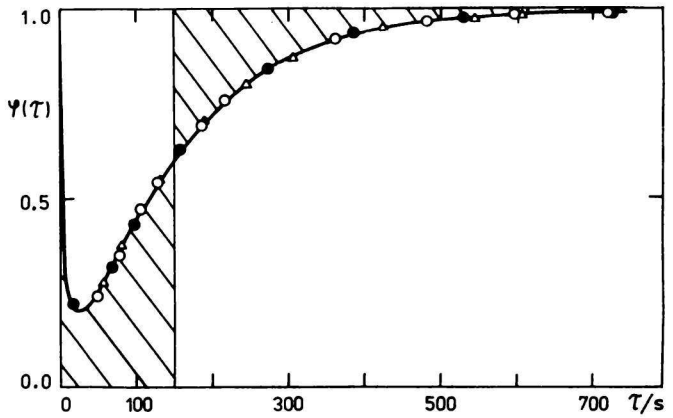

Fig. 3. Residence time distribution function in experimental device $\varphi(\tau)$.
○ Experiment 1 ; ● experiment 2 ; △ experiment 3 ; — calculated according to eqn (*5*).

The residence time distribution function $\varphi(\tau)$ is an important characteristic of the experimental device. The initial steep decrease of the function $\varphi(\tau)$, well visible from Fig. 3, is due to the joining branch between the reactor and the analyzer, the calibrated vessel and the tap for sample dosing. At the start of measurements, *i.e.* at time $\tau = 0$, the analyzer records the concentration of tracer material C_0, although the concentration is zero at the output of the reactor. After replacing the tracer material from the joining branch by the gas leaving the reactor, the analyzer starts to record the increase of its concentration. Thus the curve $\varphi(\tau)$ has a minimum.

In order to determine the mass amount $A_i(\tau)$ of the adsorbate component on the adsorbent from the experimental data we have to compute the integral (*2*) (Fig. 4). Eqn (*2*) has been solved numerically.

In this paper we present the results of sorption measurements of pure n-hexane and three mixtures of adsorptive components with different ratio of partial pressures. In all experiments the working temperature was constant, 130°C. Table 1 presents the experimental data of experiment 1, with the ratio of partial pressure of n-hexane (1) and n-heptane (2) $P_1/P_2 = 4.16$. The mass amount of the adsorbate components has to be converted to the mass per unit of the adsorbent mass

$$a_i(\tau) = \frac{A_i(\tau)}{m}$$

where m is the mass of the adsorbent.

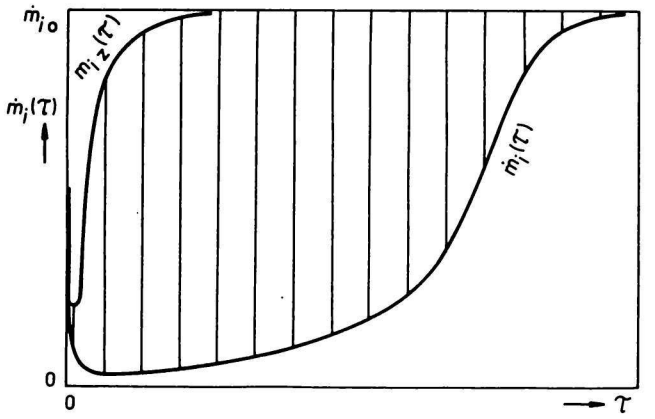

Fig. 4. Graphical method of evaluation of $A_i(\tau)$ by eqn (2).

Table 1

Experimental values of sorption measurement 1
($P_1/P_2 = 4.16$)

Reactor temperature 130°C
Pressure 97.6 kPa
Adsorbent mass 1.261 g
Mass flow of nitrogen 1.49 mg s^{-1}
Mass flow of n-hexane
28.8 μg s^{-1}
Mass flow of n-heptane
8.0 μg s^{-1}

τ/ks	$P_1(\tau)$/Pa	$c_1(\tau)$	$P_2(\tau)$/Pa	$c_2(\tau)$	$a_1(\tau)$ $\times 10^3$	$a_2(\tau)$ $\times 10^3$
0	608	1.0	146	1.0	0	0
0.39	130	0.214	11	0.077	5.5	1.8
0.98	200	0.329	18	0.121	15.3	5.2
1.57	252	0.415	27	0.187	23.8	8.3
2.14	288	0.474	36	0.247	31.0	11.1
2.67	327	0.538	43	0.291	37.1	13.6
3.30	382	0.629	52	0.357	43.0	16.3
4.10	483	0.795	63	0.430	48.4	19.4
4.75	567	0.932	70	0.478	50.5	21.6
5.58	611	1.005	78	0.533	51.0	24.2
5.82	619	1.018	81	0.555	50.9	24.9
6.53	626	1.029	88	0.604	50.5	26.8
7.25	629	1.034	95	0.648	50.0	28.5
8.35	626	1.029	104	0.712	49.2	30.7
9.43	624	1.026	112	0.769	48.5	32.5
10.61	621	1.021	120	0.821	47.8	34.1
12.02	618	1.017	129	0.886	47.2	35.4
15.21	613	1.009	141	0.967	46.3	36.7
18.91	610	1.003	144	0.987	45.8	37.3
23.86	608	1.0	146	1.0	45.7	37.5

The obtained results are graphically presented in Figs. 5—12 in the form of break-through curve (dimensionless concentration *vs.* time) and adsorption kinetic curve (adsorbed amounts $a_i(\tau)$ *vs.* time).

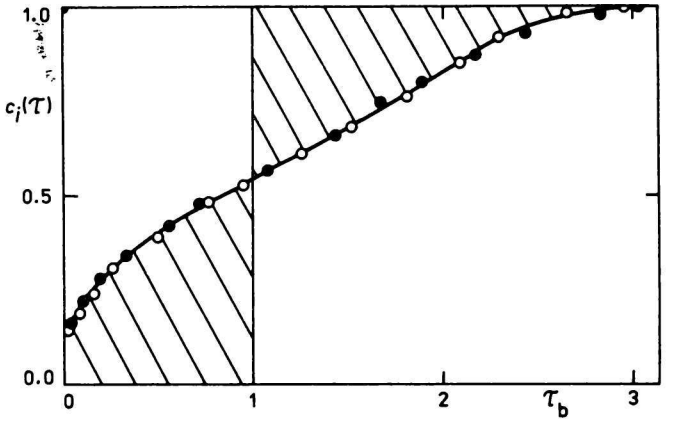

Fig. 5. Break-through curve of adsorption of n-hexane.
○ $\dot{V}_0 = 2.50$ cm^3 s^{-1}, $C_0 = 4.32$ g m^{-3};
● $\dot{V}_0 = 2.60$ cm^3 s^{-1}, $C_0 = 4.73$ g m^{-3}.

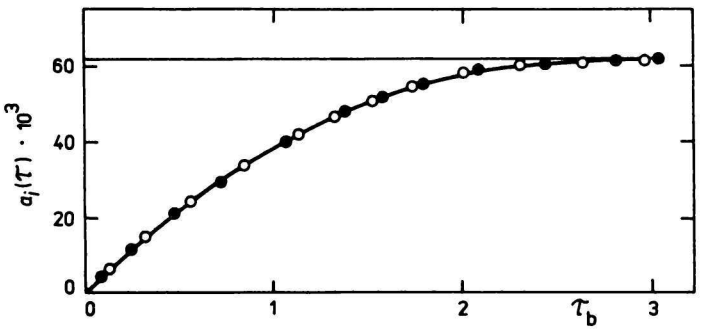

Fig. 6. Kinetic curve of adsorption of n-hexane.
○ $\dot{V}_0 = 2.50$ cm^3 s^{-1}, $C_0 = 4.32$ g m^{-3};
● $\dot{V}_0 = 2.60$ cm^3 s^{-1}, $C_0 = 4.73$ g m^{-3}.

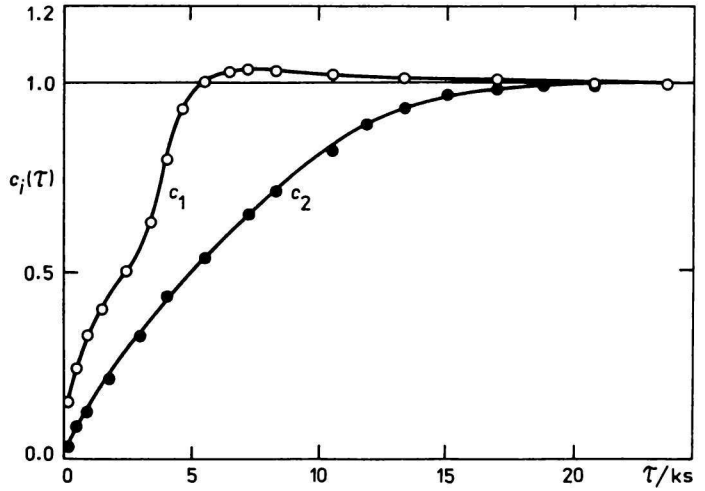

Fig. 7. Break-through curves of adsorption experiment 1 ($P_1/P_2 = 4.16$).

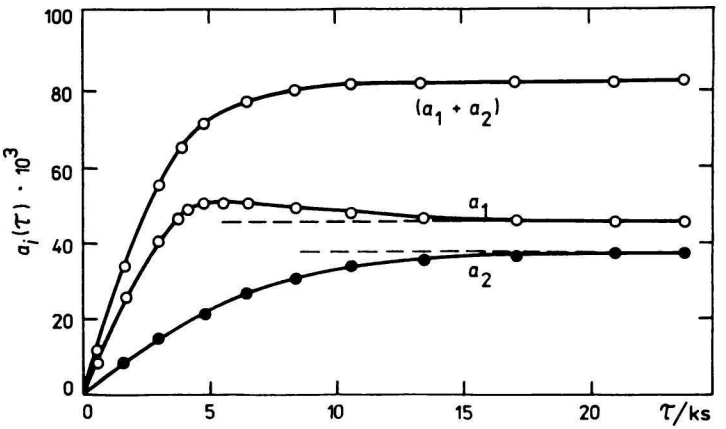

Fig. 8. Kinetic curves of adsorption experiment 1 ($P_1/P_2 = 4.16$).

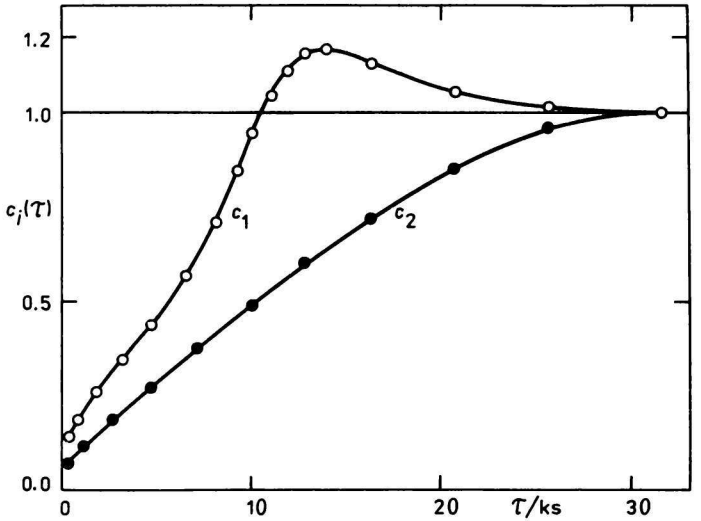

Fig. 9. Break-through curves of adsorption experiment 2 ($P_1/P_2 = 0.992$).

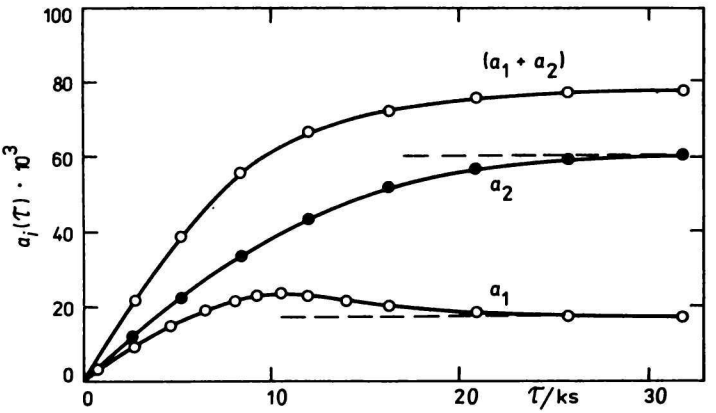

Fig. 10. Kinetic curves of adsorption experiment 2 ($P_1/P_2 = 0.992$).

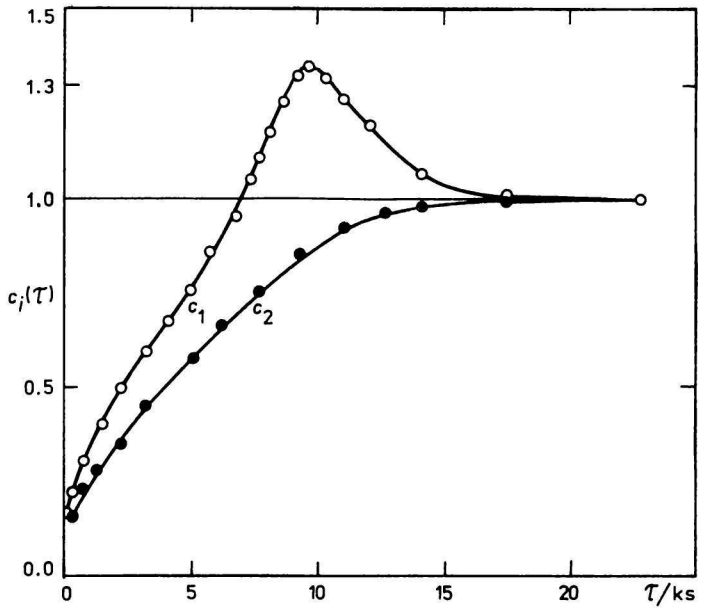

Fig. 11. Break-through curves of adsorption experiment 3 ($P_1/P_2 = 0.524$).

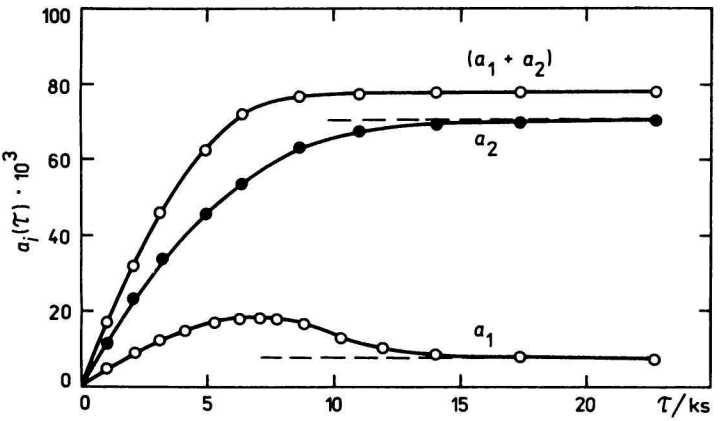

Fig. 12. Kinetic curves of adsorption experiment 3 ($P_1/P_2 = 0.524$).

Figs. 5 and 6 represent adsorption of pure component (n-hexane) for two independent experiments (empty and full circles), using close volumetric flows through the reactor and partial pressures of adsorptives. In order to be able to compare various measurements we employed dimensionless time

$$\tau_b = \frac{\tau}{\tau_k} \tag{6}$$

where τ_k represents the time in which the amount of adsorbate corresponding to the equilibrium amount on the adsorbent and in the reactor volume is introduced into the reactor. If the measurement is correct, both areas in Fig. 5 are equal. As seen from the figure, this condition is satisfied in both experiments (the deviation does not exceed 4%).

Figs. 7—12 illustrate the adsorption process for two components. For all compositions of sorption mixtures (adsorptives) replacing of the more volatile component (n-hexane) by the less volatile one is characteristic. In the beginning, when the adsorbent surface is not saturated, both components are adsorbed freely, which is reflected in the monotone increase of the adsorbed amount of both the components. During the adsorption process the degree of saturation of the adsorbent surface increases and so do the adsorbed amounts of the components on the adsorbent until equilibrium is reached. At isothermal conditions, the equilibrium amount of the adsorbate components on the adsorbent is a function of partial pressures, the ratio P_1/P_2 of which is given in the corresponding figure for each mixture. Since at the beginning of the adsorption process more amount than the equilibrium one of the volatile component is adsorbed on the free adsorbent surface, during the next period it is replaced by the second component. This phenomenon was observed in all adsorption steps. A consequence of this is a strong deformation of the shape of break-through curve compared to pure component adsorption. The most important evidence of this displacement is the maximum of the more volatile component not only on the break-through curve, but also on its kinetic curve. From Figs. 7—12 it is obvious that the displacement phase extends over a long time period, because of the slow exchange of adsorbed molecules inside of the crystal structure. This is due to the restricted volume of the intraparticle cavities of the molecular sieve. It is interesting that the interval of displacement of the more volatile component is several times longer than the adsorption interval. Also, it is interesting that the value of the maximum which is higher than the equilibrium one increases with the decrease of the partial pressure ratio P_1/P_2.

The rate of adsorption

Based on the experimental data of the adsorption kinetics, which are illustrated in Figs. 8, 10, 12 as a function

$$a_i = a_i(\tau) \tag{7}$$

we can also express the rate of adsorption $r_i(\tau)$ as a function of relative adsorbed amount $\alpha(\tau)$

$$r_i(\tau) = r_i[\alpha(\tau)] \tag{8}$$

The rate of adsorption is evaluated from the experimental data. For the experiment 1 the resulting adsorption rates (together with further quantities according to eqns (*9*) and (*10*)) are in Table 2.

The results are illustrated in Fig. 13. The abscissa is the relative adsorbed amount

$$\alpha(\tau) = \frac{a(\tau)}{a} = \frac{a_1(\tau) + a_2(\tau)}{a_1 + a_2} \tag{9}$$

where a is the equilibrium mass amount of the adsorbate on the adsorbent and $a(\tau)$ is the mass amount of the adsorbate in time τ.

Table 2

Rate of adsorption of the components $r_i(\tau)$ *vs.* relative adsorbed amount $\alpha(\tau)$ for experiment 1

τ/ks	$a_1(\tau)$ $\times 10^3$	$a_2(\tau)$ $\times 10^3$	$\Sigma a_i(\tau)$ $\times 10^3$	$\alpha(\tau)$	$r_1(\tau)$ $10^6 \cdot s^{-1}$	$r_2(\tau)$
0	0	0	0	0	0	0
0.27	3.5	1.1	4.6	0.055	17.4	6.09
0.50	7.5	2.5	10.0	0.120	16.4	5.56
0.86	13.4	4.5	17.9	0.215	15.3	5.33
1.16	18.0	6.1	24.1	0.290	14.0	5.33
1.46	22.2	7.7	29.9	0.360	13.9	5.22
1.69	25.4	8.9	34.3	0.412	12.4	4.89
2.14	31.0	11.1	42.1	0.506	11.5	4.71
2.67	37.1	13.6	50.7	0.609	9.37	4.28
3.30	43.0	16.3	59.3	0.713	7.73	4.09
3.74	46.4	18.1	64.5	0.775	4.06	3.47
4.75	50.5	21.6	72.1	0.867	0.83	3.33
5.23	50.9	23.2	74.1	0.891	0.29	2.86
5.58	51.0	24.2	75.2	0.904	−0.42	2.92
5.82	50.9	24.9	75.8	0.911	−0.56	2.68
6.53	50.5	26.8	77.3	0.929	−0.69	2.36
7.25	50.0	28.5	78.5	0.944	−0.73	2.00
8.35	49.2	30.7	79.9	0.960	−0.62	1.50
10.61	47.8	34.1	81.9	0.984	−0.37	0.74
13.60	46.7	36.3	83.0	0.998	−0.10	0.12
23.86	45.7	37.5	83.2	1.000		

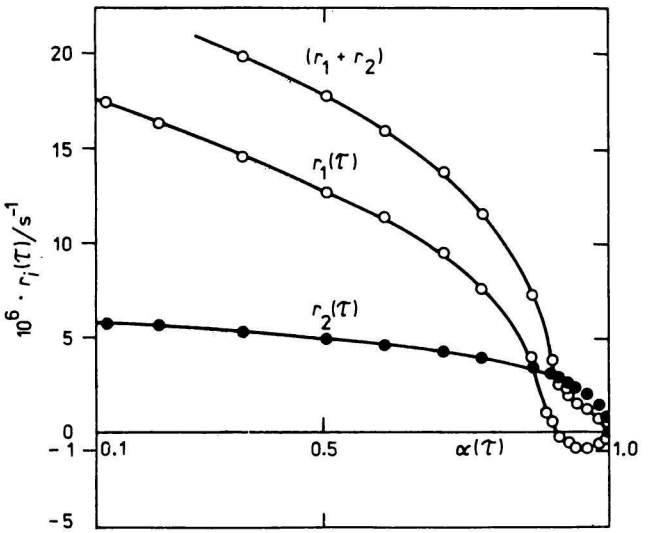

Fig. 13. Rate of adsorption of components *vs.* relative adsorbed amount — experiment 1 ($P_1/P_2 = 4.16$).

The ordinate is the rate of adsorption of the component $r_i(\tau)$

$$r_i(\tau) = \frac{da_i(\tau)}{d\tau} \tag{10}$$

By the same method also the experimental data for the remaining mixtures have been processed. The results are illustrated in Figs. 14 and 15.

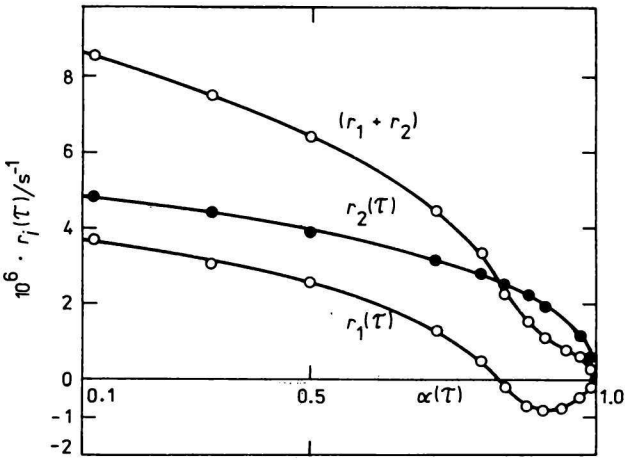

Fig. 14. Rate of adsorption of components *vs.* relative adsorbed amount — experiment 2 ($P_1/P_2 = 0.992$).

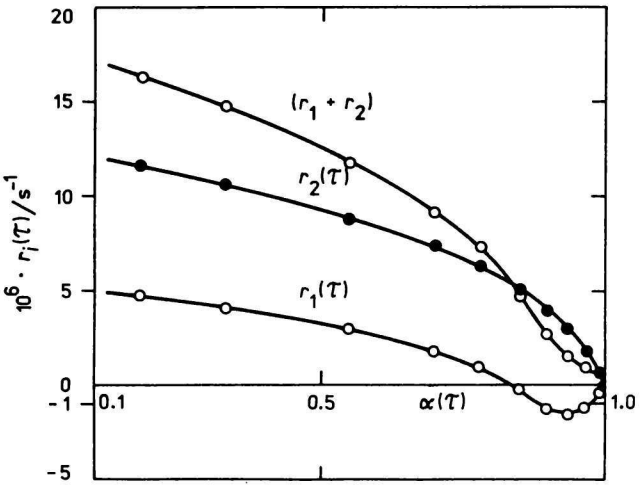

Fig. 15. Rate of adsorption of components *vs.* relative adsorbed amount — experiment 3 ($P_1/P_2 = 0.524$).

A characteristic feature for all dependences is the decrease of adsorption rate of the more volatile component $r_1(\tau)$ down to negative values, which actually correspond to desorption, *i.e.* displacement of the more volatile component by the less volatile one.

At equilibrium when the driving force is zero, the adsorption rate is, of course, also zero and the relative adsorbed amount is $\alpha = 1$.

Near the equilibrium on the almost saturated adsorbent surface the adsorbate molecules take their equilibrium placements while the adsorption rate is very low. As seen from Table 2, the time required for 90% saturation of the adsorbent is about three times shorter than for the settling down to equilibrium, which is associated with the saturation of the last 10% of the adsorbent capacity. Similar relations were observed also for other mixtures.

Symbols

a equilibrium mass of the adsorbate mixture per mass adsorbent unit
a constant in eqn (*5*)
a_i equilibrium mass of the i-th adsorbate component per mass adsorbent unit
$a_i(\tau)$ mass of the i-th adsorbate component per mass adsorbent unit at time τ
$A_i(\tau)$ mass of the i-th adsorbate component at time τ
b constant in eqn (*5*)
c constant in eqn (*5*)

$c_i(\tau)$ dimensionless concentration of the i-th component in the gas stream
$C_i(\tau)$ concentration of the i-th component in the gas stream leaving the reactor
C_{i0} concentration of the i-th component in the gas stream entering the reactor (during adsorption step constant)
C_{i0n} equilibrium concentration of the i-th component corresponding to the previous step
m adsorbent mass
$\dot{m}_{i0}$ mass flow of the i-th component in the gas stream entering the reactor (corresponding to the concentration C_{i0})
$\dot{m}_i(\tau)$ mass flow of the i-th component in the gas stream leaving the reactor
$\dot{m}_{iz}(\tau)$ mass flow of the i-th component in the gas stream leaving the reactor, provided no adsorption is taking place
P_i partial pressure of the i-th component of the gas adsorptive
$r_i(\tau)$ rate of adsorption of the i-th component
τ time
τ_b dimensionless time of adsorption
$\dot{V}_0$ volumetric gas flow of the adsorptive mixture
$\alpha(\tau)$ relative adsorbed amount given by eqn (*9*)
$\varphi(\tau)$ residence time distribution function

References

1. Ilavský, J. and Longauer, J., *Chem. Zvesti 32*, 145 (1978).
2. Ilavský, J. and Longauer, J., *Ropa Uhlie 15*, 233 (1973).
3. Gast, T., *Feinwerktechnik 53*, 167 (1949).
4. Smith, J. M., *Chemical Engineering Kinetics*. McGraw-Hill, New York, 1970.
5. Robens, E. and Sandstede, G., *Gravimetrischer Sorptionsautomat*. Frankfurt/Main, 1967.
6. Bronštejn, I. N. and Semendajev, K. A., *Príručka matematiky*. (A Handbook of Mathematics.) Slovenské vydavateľstvo technickej literatúry. (Slovak Publishing House of Technical Literature.) Bratislava, 1964.

Translated by P. Brunovský